Available online at www.sciencedirect.com

ScienceDirect

Energy Procedia 4 (2011) 5122–5129

Energy Procedia

www.elsevier.com/locate/procedia

GHGT-10

Corrosion behaviour of pipe steels exposed for 2 years to CO_2-saturated saline aquifer environment similar to the CCS-site Ketzin, Germany

Anja Pfennig[a]*, Barbara Linke[a] and Axel Kranzmann[b]

[a]*HTW University of Applied Sciences Berlin, Wilhelminenhofstraße 75 A, Gebäude C, 12459 Berlin, Germany*

[b]*BAM Federal Institute of Materials Research and Testing, Unter den Eichen 87, 12205 Berlin, Germany*

Abstract

When emission gasses are compressed into deep geological layers (CCS) CO_2-corrosion of injection pipe steels is a relevant safety issue. The reliability of the steels used at the geological onshore CCS-site at Ketzin, Germany, is demonstrated in 2 years laboratory experiments under an equivalent corrosive environment at ambient pressure (T=60 °C, aquifer water, CO_2-flow rate of 3 l/h). Corrosion kinetics and microstructures were characterized using samples of the heat treated steel 42CrMo4 (casing), and samples of the martensitic stainless steel X46Cr13 (injection).

Keywords: steel; pipeline; corrosion; CCS; CO_2-storage

1. Introduction

When compressing CO_2 into the deep geological layers of the Carbon Capture and Storage (CCS)-site Ketzin, Germany (CO_2-SINK [1,2]) corrosion of the casing and injection pipe steels may become an issue because CO_2-corrosion is sensitively dependent on alloy composition, contamination of alloy and media, environmental conditions like temperature, CO_2 partial pressure, flow conditions and protective corrosion scales [3-8]. During the injection period the CO_2 or emission gasses are kept within one phase (liquid or supercritical). But during injection discontinuation and in the time after the injection phase the humidity will increase within the borehole and might cause severe corrosion damage to the steels. The Ketzin temperature regime between 40 °C to 60 °C is critical well known for severe corrosion processes as shown by various authors [8-10]. Pfennig and Bäßler demonstrate that the worst intrusion depth for pit corrosion of 13% Cr steel X46Cr13 has a maximum around 4.7 mm/year [11] but may also be predicted by the rather conservative Norsok-Model for the oil and gas industry [12]. As found in pits of locally corroded samples [26] steels exposed to CO_2-environment generally precipitate slow growing non passivating surface layers mainly comprised of $FeCO_3$ (siderite) [9,10,13-16].

* Corresponding author. Tel.: +49 30 8104 3119; fax: +49 30 8104 1517.
E-mail address: anja.pfennig@htw-berlin.de.

doi:10.1016/j.egypro.2011.02.488

2. Materials and Methods

Exposure tests in CO_2-saturated aquifer brine were carried out using samples made of thermally treated specimen of steels (8x20x50 mm^3) with 1% Cr 42CrMo4 (1.7225, AISI 4141), and 13% Cr X46Cr13 (1.4034, AISI 420). The surfaces were activated by grinding with SiC-Paper down to 120 µm under water. Samples of each base metal were positioned within the vapour phase, the intermediate phase with a liquid/vapour boundary and within the liquid phase [8]. The brine (as known to be similar to the Stuttgart Aquifer [17]: Ca^{2+}: 1760 mg/L, K^{2+}: 430 mg/L, Mg^{2+}: 1270 mg/L, Na^{2+}: 90.100 mg/L, Cl^-: 143.300 mg/L, SO_4^{2-}: 3600 mg/L, HCO_3-: 40 mg/L) was synthesized in a strictly orderly way to avoid precipitation of salts and carbonates. Flow control (3 NL/h) of the technical CO_2 into the brine was done by a capillary meter GDX600_man by QCAL Messtechnik GmbH, München. The pH after the experiments was between 5.2 and 5.6. The heat treatment of the samples between 700 h to 17520 h was disposed in a chamber kiln according to the conditions at the geological site at Ketzin/Germany at 60 °C at ambient pressure – each material in a separated reaction vessel. X-ray diffraction was carried out in a URD-6 (Seifert-FPM) with CoKα-radiation with an automatic slit adjustment, step 0.03 and count 5 sec. Phase analysis was performed by matching peak positions automatically with PDF-2 (2005) powder patterns. Mainly structures that were likely to precipitate from the steels were chosen of the ICSD and refined to fit the raw-data-files using POWDERCELL 2.4 [18] and AUTOQUAN ® by Seifert FPM.

Descaling of the samples was performed by exposure to 37% HCl for 24 hours and mass gain was analyzed according to DIN 50 905 part 1-4. Non descaled parts of the samples were embedded in a cold resin (Epoxicure, Buehler), cut and polished first with SiC-Paper from 180 µm to 1200 µm under water and then finished with diamond paste 6 µm, 3 µm and 1 µm. The measurement of the layer thicknesses and residual pipe wall thicknesses was performed via light and electron microscopy techniques using the semi-automatic analyzing program Analysis Docu ax-4 by Aquinto. A set of 100 linescans were measured taking a set of 10 to 20 micrographs per parameter.

3. Results and Discussion

Figure 1 illustrates the samples 42CrMo4 and X46Cr13 after 2 years of exposure to the CO_2-saturated saline aquifer water. The severe corrosion layer is clearly visible on the samples kept within the vapour phase. This is also demonstrated on the etched surfaces of the samples where holes and flaws reduce the thickness of the base materials.

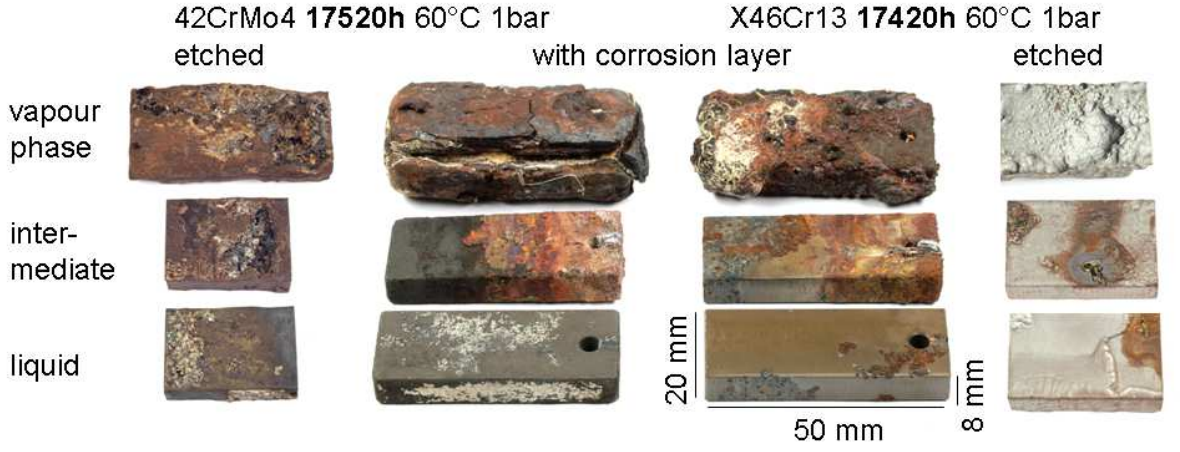

Figure 1: Surface images of the samples 42CrMo-4 and X46Cr13 after 2 years of exposure to the CO2-saturated saline aquifer water at 60 °C and ambient pressure.

3.1. Kinetics of surface corrosion

The isothermal oxidation behaviour of the alloys X46Cr13 and 42CrMo4 at 60 °C/ambient pressure characterized by mass gain according to DIN 905 part 1-4 is illustrated by figure 2. The greatest corrosion rates are generated when the samples are exposed to the vapour phase, the lowest when exposed to the liquid phase. The greatest increase of the corrosion rates up to 2000 h is correlated to the growth of siderite $FeCO_3$ in CO_2-atmosphere. After 1 year a steady corrosion rate is achieved where the loss of base material can be predicted in from a constant corrosion rate. This is 0.8 mm/year for 42CrMo4 and 0.35 mm/year for X46Cr13 when exposed to the H_2O-saturated CO_2 (vapour phase) and approximately 0.15 mm/year for both steels when exposed to the intermediate and the liquid phase. In general the corrosion rate increases with increasing CO_2 partial pressure, but in the presence of iron carbonate precipitates (siderite) the corrosion rate may even decrease and is the reason for the steady corrosion rates at longer exposure times.

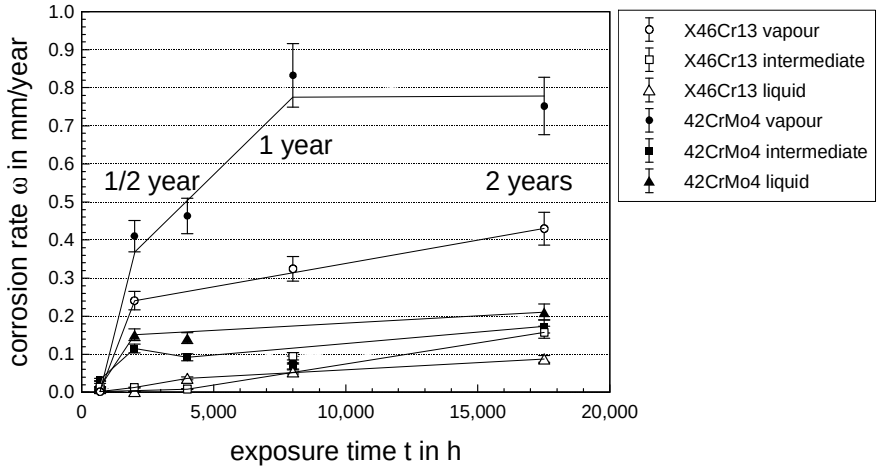

Figure 2: Corrosion rate as a function of exposure time of the alloys X46Cr13 and 42CrMo4 (60 °C / CO_2 saturated brine / ambient pressure).

Figure 3 shows the loss of pipe wall thickness as a function of heat treatment in CO_2 saturated brine at 60 °C and ambient pressure measured metallographically. The tops and bottoms of the error bars indicate highest and lowest measured value. Samples kept in the vapour phase show greater loss in wall thickness than samples kept in the intermediate and liquid phase. The loss of wall thickness of 42CrMo4 is 2 to 3 times higher than the loss of X46Cr13. The locally measured loss in wall thickness as demonstrated is higher almost by a factor of 2 than predicted by mass loss.

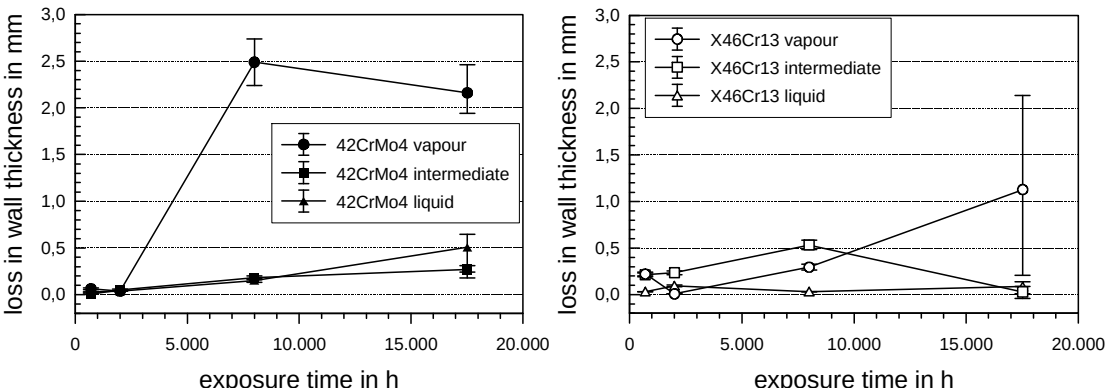

Figure 3: Loss of pipe wall thickness as a function of heat treatment measured metallographically (tops and bottoms of error bars indicate highest and the lowest measured value).

3.2. Kinetics of corrosion layer

In good agreement to the corrosion rate obtained from mass gain and loss of wall thickness the growth of the scale thicknesses is much greater within the vapour phase than in the intermediate and liquid phase (figure 6). (Here again the tops and bottoms of the error bars indicate the highest and the lowest measured value.) This can be explained by the easier access of CO_2 through the porous corrosion layer and the higher partial pressure of oxidizing medium in the vapour phase. Here the CO_2 steam is saturated with H_2O in contrast to the liquid H_2O saturated with CO_2. Specimens in the intermediate phase show the typical corrosion scale of the media it was exposed to but neither enhancement nor reduction of the corrosion rates were found.

Thicknesses of the corrosion layers found on 42CrMo4 are nearly the same for X46Cr13 when the samples are kept in the liquid and intermediate phase. The scale thicknesses are of 0.3 mm magnitude regardless of the exposure time. But 42CrMo4 kept in the vapour phase shows a great increase in layer thickness within the first year (8000 h) to then steady at about 6 mm layer magnitude. The increase in layer thickness of X46Cr13 is not as significant as that of 42CrMo4, but also shows a plateau after 1 year of exposure at 2.8 mm layer magnitude. With longer exposure time the difference between the highest and the lowest thickness measured increases, meaning that while the overall layer thickness may be constant after an initiation time of approximate 1 year certain layer areas may be much smaller or much larger.

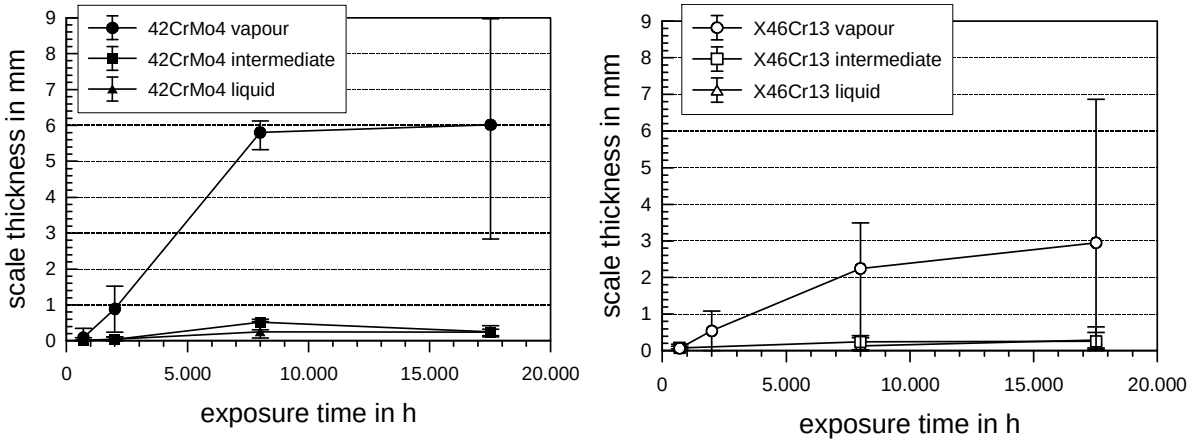

Figure 6: Scale thickness of the alloys 42CrMo4 (left) and X46Cr13 (right) as a function of exposure time in CO_2-satured brine at 60°C and ambient pressure.

The kinetics of local corrosion is described in detail by Pfennig and Kranzmann [38].

Relating to the worst case of a water level rising within the pipes and sitting there for two years the following conclusion may be drawn: Both, surface corrosion as well as local corrosion (pitting and shallow pit corrosion), contribute to the degradation of the pipeline material. Considering pitting the highest intrusion rates are obtained for the high chromium steel X46Cr13 (4.6 mm/year [11]) whereas surface corrosion rates are lowest around 0.4 mm/year (by mass gain) or show a 2 mm loss in wall thickness after 2 years of exposure. After 2 years of exposure to a H_2O saturated CO_2 surface corrosion rates of 42CrMo4 are much higher (0.8 mm/year by mass gain) and a loss in wall thickness determined metallographically of 2.5 mm/year.

3.3. Microstructure.

Figure 7 reveals typical corrosion layer surfaces grown on 42CrMo-4 and X46Cr13. Salts from reactions of alloying elements, iron with the brine are visible as well as oxides, hydroxides and carbonates. The needle-shaped precipitates are identified as iron oxides and the cubic precipitates

are halites NaCl. Typical phases of the complicated multilayer scale (figure 8) are given in table 1:

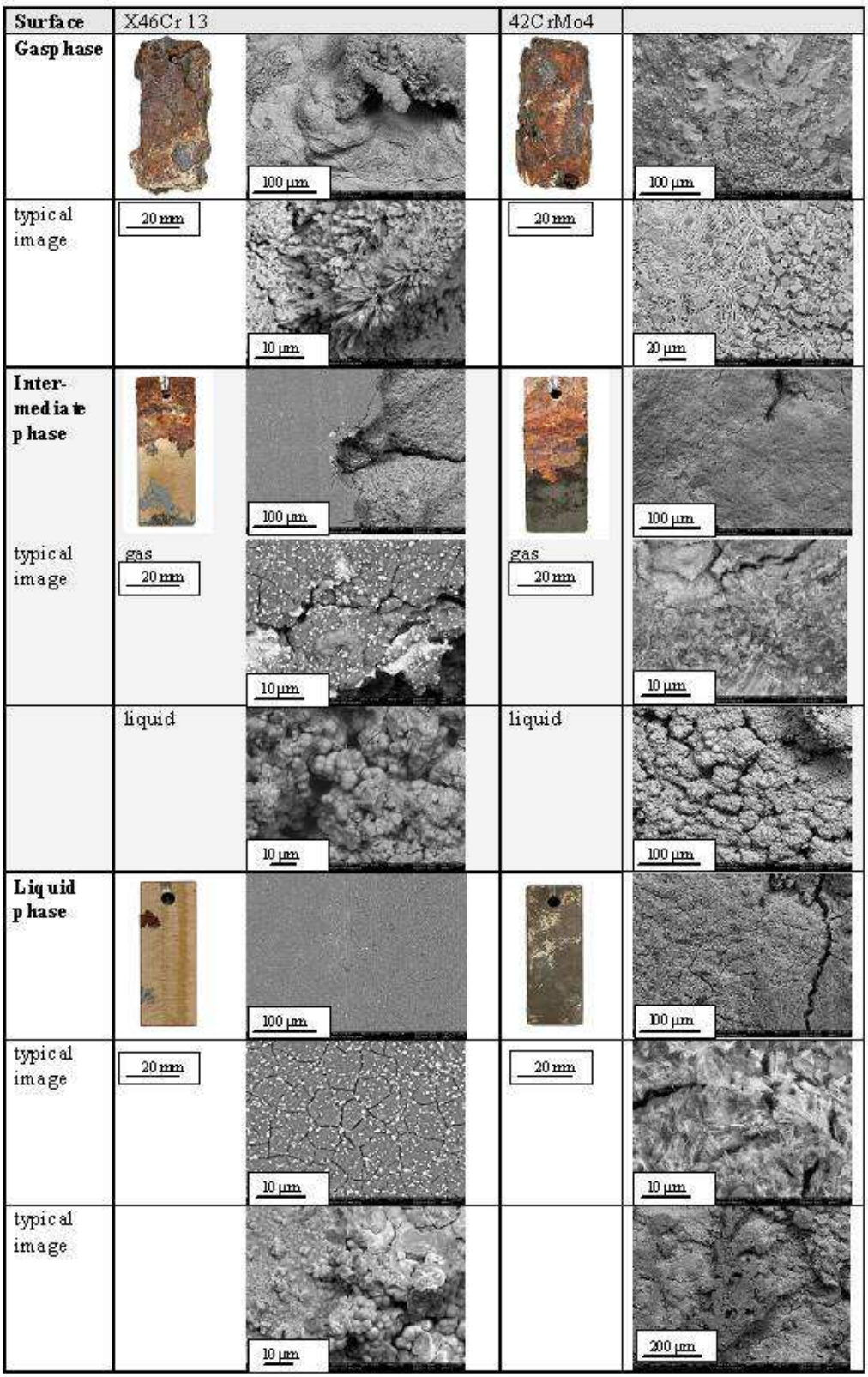

Figure 7: SEM surface images of the corrosion scale on the alloys X46Cr13 (left) and 42CrMo4 (right) as a function of exposure time in CO_2-satured brine at 60°C and ambient pressure.

Table 1: Typical phases found on the steels analyzed by XRD

Phase[a]	X46Cr13			42CrMo4		
	vap[b]	int	liq	vap	int	liq
Siderite	x[c]	x		x	x	x
Geothite	X	X		X	X	
Magnetite	x	x		x	x	
Rhodochrosite	x	x		x	x	x
Hematite	x	x		x	x	
Akaganeite				X	X	X
Mackinawite	x	x		x	x	
Chromite		x		x	x	x
Chromium				x		x
Cementite					X	X
$Fe_{2,7}Mn_3C$					X	X
Mn_5C_2	X					X
Lepidocrocite		X				
Halite, Eskolaite		x				

[a] Siderite $FeCO_3$; Geothite FeOOH; Magnetite Fe_3O_4; Rhodochrosite $MnCO_3$; Hematite Fe_2O_3; Akaganeite $Fe_8(O,OH)_{16}Cl_{1.35}$; Mackinawite FeS; Chromite $FeCr_2O_4$; Chromium $Cr_{1.3}Fe_{0.7}O_3$; Cementite Fe_3C, Eskolaite Cr_2O_3

[b] vap- vapour; int-intermediate; liq-liquid

[c] X- main phases; x- minor phases

42CrMo4. Figure 8 shows a corrosion layer of 42CrMo-4 after 2 years of heat treatment at 60 °C in saline aquifer brine with typical duplex structure revealing the outer and the inner layer. The total layer thickness varies from 20 µm to 6000 µm. Samples in the intermediate phase show cavities with a depth about 50 µm and a width of 200 µm. After 2 years of exposure the thickness of the outer layer varies significantly. It can rise up to 6 mm in the vapour phase and after 4000 h even a small inner layer is connected to 3-4 mm outer layer. Its thickness increases significantly with heat treatment from 8000 h to 17520 h. Mainly consisting of the inner layer the corrosion layer thickness of samples in the liquid phase is around 500 µm. Precipitates of the oxides are mainly needle-shaped, those of the salts are either needles or blocks and the entire corrosion layer summing inner and outer layer is highly porours and therefore non passivating.

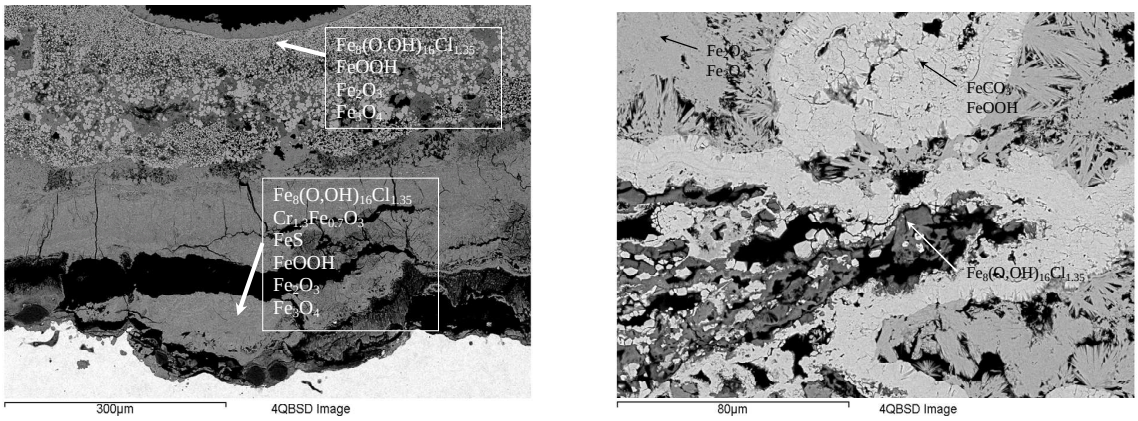

Figure 8: Corrosion layer and phases of 42CrMo4 after 2 years (17520 h) of heat treatment in CO_2 saturated brine at ambient pressure kept in the vapour phase (H_2O saturated CO_2).

X46Cr13. X46Cr 13 shows surface corrosion with a typical duplex layer formation as states for the 1%Cr steel. Also the thickness of the corrosion layer in the vapour phase is much greater than in the intermediate and especially in the liquid phase. After 17520 h exposure time at ambient pressure an outer corrosion layer is strongly visible in the vapour and the intermediate phase that grows to 3.5 mm within the vapour phase. Also an inner layer up to 1200 µm has grown while the liquid phase shows little to no surface corrosion (Figure 9). The precipitation mechanism is described in detail by Pfennig, Bäßler and Kranzmann [26,27].

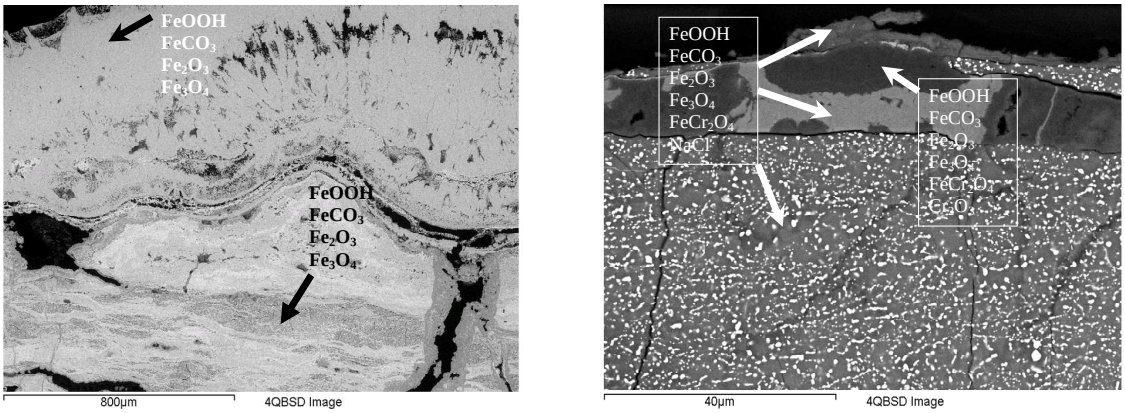

Figure 9: Corrosion layer and phases of X46Cr13 after 2 years (17520 h) of heat treatment in CO_2 saturated brine at ambient pressure (left: vapour phase, right: intermediate phase).

As the multiphase corrosion layer grows it reaches an equilibrium thickness after approximately one year of exposure. After this time the layer thickness increases further but becomes denser, therefore less porous. This means that the mutual diffusion of Fe from the base metal and O_2, C and impurities from the CO_2-saturated brine is slowed down resulting in a stable corrosion layer growth and base metal dissolution.

4. Conclusion

Highest surface corrosion rates obtained by mass gain are 0.8 mm/year (1% Cr (42CrMo-4)) and 0.35 mm/year (13% Cr (X46Cr13)) in the vapour phase. The average intermediate and liquid corrosion rate for both type of steel is 0.1 mm/year, while pits may be as deep as 4.7 mm [11]. The complex continuous scale of both types of steel is comprised of $FeCO_3$ siderite, FeOOH goethite and FeS mackinawite, spinelphases of various compositions and akaganeite $Fe_8O_8(OH)_8Cl_{1.34}$. When there are intermissions of the injection it is highly recommended that the borehole is kept under pressure and inert gas phases to keep the aquifer water from rising in the injection pipe. If there is an aquifer water level in the borehole the initiation of pit formation and a fast surface degradation of the pipe parts above the water level become very likely. Besides the loss in wall thickness and associated loss in tensile strength there is the likeliness of parts of the scale falling down into the injection pipe part (figure 10). Initiated from pits the loss of pipe wall may proceed in a lateral way leading to the connection of injection holes. Imagining the worst case these may connect and then parts of the pipe may be lost as demonstrated in figure 10. But following from the obtained corrosion rates the steels used for injecting technical CO_2 in Ketzin will withstand at least a 2 year period of injection without a need of replacement if the tensile stresses can be reduced to a minimum and the decrease in pressure along the pipe wall cross section is kept low.

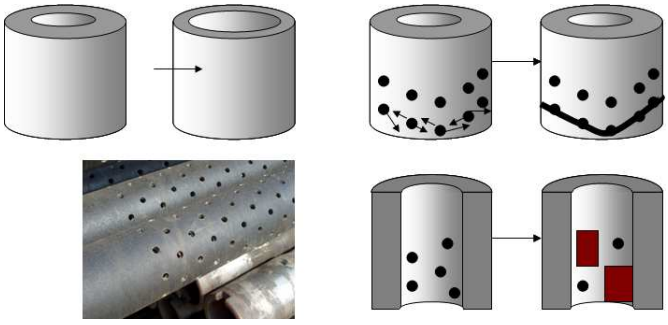

Figure 10: Corrosion layer and phases of X46Cr13 after 2 years (17520 h) of heat treatment in CO_2 saturated brine at ambient pressure (left: vapour phase, right: intermediate phase).

5. Acknowledgement

This work was supported by the FNK (Fachkonferenz für wissenschaftlichliche Nachwuchskräfte) of the Applied University of Berlin, HTW and by IMPACT (EU-Project EFRE 20072013 2/21).

6. References

[1] D.C. Thomas, Carbon Dioxide Capture for Storage in Deep Geologic Formations – Results from CO_2 Capture Project, Volume 1: Capture and Separation of Carbon Dioxide form Combustion Sources, CO_2 Capture Project, Elsevier Ltd UK 2005, ISBN 0080445748

[2] GeoForschungszentrum Potsdam, CO_2-SINK – drilling project, description of the project PART 1 (2006) 1-39

[3] Z.D. Cui, S.L. Wu, S.L. Zhu, X.J. Yang, Study on corrosion properties of pipelines in simulated produced water saturated with supercritical CO_2, Appl. Surface Science 252 (2006) 2368-2374

[4] D.A. Lopez, T. Perez, S.N. Simison, The influence of microstructure and chemical composition of carbon and low alloy steels in CO_2 corrosion, Materials and Design 24 (2003) 561-575

[5] L.J. Mu, W.Z. Zhao, Investigation on Carbon Dioxide Corrosion Behaviors of 13Cr Stainless Steel in Simulated Strum Water, Corrosion Science, Manuscript No. CORSCI-D-09-00353 (2009) 1-24

[6] H. Zhang, Y.L Zhao, Z.D. Jiang, Effects of temperature on the corrosion behaviour of 13Cr martensitic stainless steel during exposure to CO_2 and Cl^- environment, Material Letters 59 (2005) 3370-3374

[7] Y.-S. Choi and S. Nešić, Corrosion behaviour of carbon steel in supercritical CO_2-water environments, Paper No. 09256, NACE Corrosion 2008 Conference and Expo, New Orleans, Louisiana, USA, March 16th – 20th, 2008

[8] Pfennig, A., Bäßler, R. "Effect of CO_2 on the stability of steels with 1% and 13% Cr in saline water" Corrosion Science, Vol. 51, Issue 4 (2009) 931-940

[9] D.S. Carvalho, C.J.B. Joia, O.R. Mattos, Corrosion rate of iron and iron-chromium alloys in CO_2-medium, Corrosion Science 47 (2005) 2974-2986

[10] B.R. Linter, G.T Burstein, Reactions of pipeline steels in carbon dioxide solutions, Corrosion Science 41 (1999) 117-139

[11] Pfennig, A., Kranzmann, A., The role of pit corrosion in engineering the carbon storage site Ketzin, Germany, Air Pollution 21st -23rd June 2010, Kos, Greece

[12] http://www.standard.no/pronorm-3/data/f/0/01/36/9_10704_0/M-506d1r2.pdf,"C_{O2} corrosion rate calculation model"

[13] J. Han, Y. Yang, S. Nešić, B. N. Brown, Roles of passivation and galvanic effects in localized CO_2 corrosion of mild steel, Paper No. 08332, NACE Corrosion 2008 Conference and Expo, New Orleans, Louisiana, USA, March 16th – 20th, 2008

[14] S.L Wu, Z.D. Cui, F. He, Z.Q. Bai, S.L. Zhu, X.J. Yang, Characterization of the surface film formed from carbon dioxide corrosion on N80 steel, Materials Letters 58 (2004) 1076-1081

[15] D.A. Lopez, W.H. Schreiner, S.R. de Sánchez, S.N. Simison, The influence of carbon steel microstructure on corrosion layers, Applied Surface Science 207 (2003) 69-85

[16] Banaś, U. Lelek-Borkowska, B. Mazurkiewicz, W. Solarski, Effect of CO_2 and H_2S on the composition and stability of passive film on iron alloy in geothermal water, Electrochimica Acta 52 (2007) 5704-5714

[17] A. Förster et al., 2006, Baseline characterization of the CO_2SINK geological storage site at Ketzin, Germany: Environmental Geosciences, V. 13, No. 3 (September 2006), pp. 145-161.

[18] SW. Kraus and G. Nolze, POWDER CELL, J. Appl. Cryst. (1996), 29, 301-303